Micro-arrow sensor array with enhanced skin adhesion for transdermal continuous monitoring of glucose and reactive oxygen species
Supplementary Information

Xinshuo Huang,[1,+] Baoming Liang,[1,+] Shantao Zheng,[1] Feifei Wu,[1,3] Mengyi He,[1] Shuang Huang,[1] Jingbo Yang,[2] Qiangqiang Ouyang,[4] Fanmao Liu,[4] Jing Liu,[4] Hui-jiuan Chen,[1,*] Xi Xie[1,2,*]

[1]State Key Laboratory of Optoelectronic Materials and Technologies, School of Electronics and Information Technology; Guangdong Province Key Laboratory of Display Material and Technology, Sun Yat-Sen University, Guangzhou, China

[2]School of Biomedical Engineering, Sun Yat-Sen University, Guangzhou, China

[3]Pazhou Lab, Guangzhou 510330, China

[4]The First Affiliated Hospital of Sun Yat-Sen University, Guangzhou, China

* Corresponding authors, E-mail:

chenhuix5@mail.sysu.edu.cn, xiexi27@mail.sysu.edu.cn

+These authors contributed equally to this work.

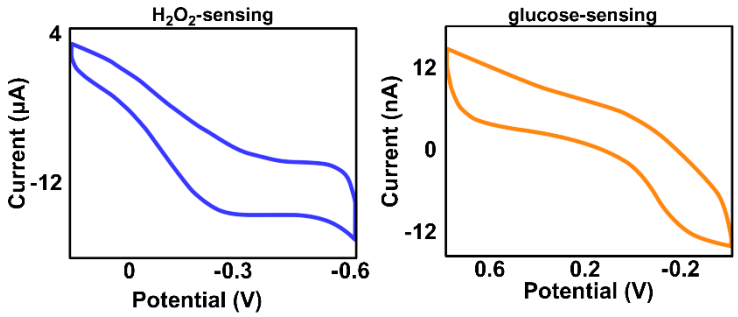

Figure S1. Cyclic voltammetric curves (CVs) of metabolite sensing electrodes in 0.1 mol/L phosphate (PBS) buffer solution, including the current response of H_2O_2 sensing electrodes (H_2O_2) and glucose sensing electrodes (glucose)

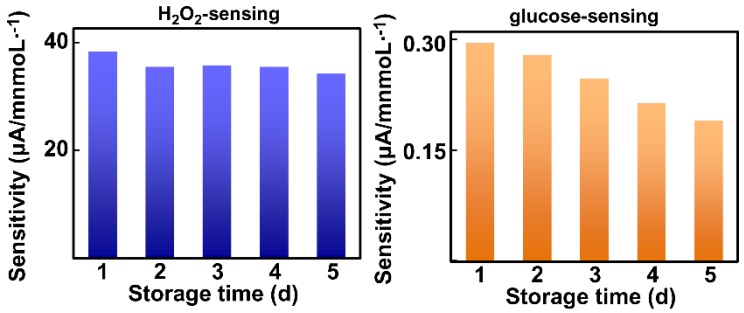

Figure S2. Graphs showing the reproducibility characteristics of the metabolite sensing micro-arrow electrodes over the course of a week. Daily sensitivity changes were estimated for each electrochemical sensor over the week. The sensitivity changes were calibrated for each subsequent day by testing different electrodes before setting the sensitivity on day 1 to a baseline value of 100%. The results showed that the H_2O_2 sensing electrode maintained excellent temporal stability, while the glucose sensing electrode showed a significant change in sensitivity that was difficult to ignore from day 3 onwards. As shown above, the final relative sensitivities of these sensors after 4 days were 89.3% for the H_2O_2-sensing electrode and 64.2% for the glucose-sensing electrode. The sensitivity of the metabolite-sensing micro-arrow electrodes remained stable during 4 days of storage, demonstrating the importance of pre-calibration to improve sensor stability.

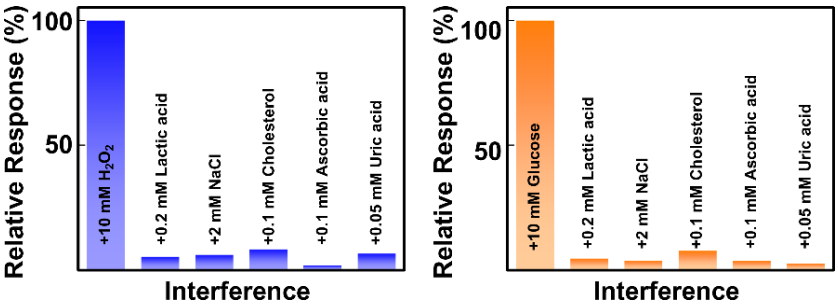

Figure S3. Graphs showing the selectivity (relative values) of the metabolite sensing micro-arrow electrode for H_2O_2 and glucose sensing. The selectivity of the electrode detection was tested by sequentially adding 10 mM H_2O_2, 0.2 mM lactate, 2 mM NaCl, 0.1 mM cholesterol, 0.1 mM ascorbic acid and 0.05 mM uric acid to the test solution of the H_2O_2-sensing micro-arrow electrode. For better discussion, response signal of the first time was regarded as 100% after which the later signals were normalized, converted into relative values. Results suggested that the H_2O_2-sensing micro-arrow electrode exhibited a significant current signal only for the presence of H_2O_2, while the presence of interfering substances such as lactic acid, sodium chloride, cholesterol, ascorbic acid and uric acid produced only a very weak voltage signal (< 8%) for the electrode. Results above demonstrated that the H_2O_2-sensing micro-arrow electrode could selectively detect H_2O_2 concentration and avoid interference from other substances.

Similarly, the selectivity of the glucose-sensing micro-arrow electrode was tested by sequentially adding 10 mM glucose, 0.2 mM lactic acid, 2 mM sodium chloride, 0.1 mM

cholesterol, 0.1 mM ascorbic acid and 0.05 mM uric acid to the test solution of the glucose-sensing micro-arrow electrode. The results indicated that the glucose-sensing micro-arrow electrode processed a significant current signal only for the presence of glucose, while weak voltage signals (<8%) only occurred with the presence of interferents such as lactic acid, sodium chloride, cholesterol, ascorbic acid and uric acid. These results demonstrated that the glucose-sensing micro-arrow electrode could achieve specific detection of glucose with the interference of other substances.

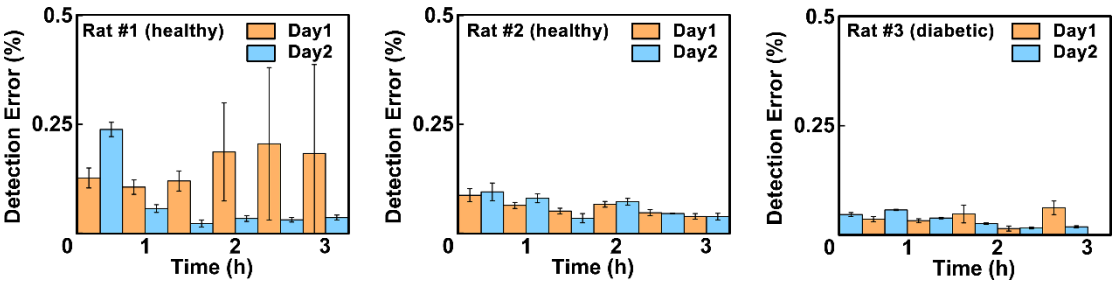

Figure S4. Rats (N=3) were monitored continuously in vivo for 3 hours over 2 days using metabolite-sensing micro-arrow electrodes and the measured glucose concentrations were calibrated with the measured H_2O_2 concentrations. Graphs above showed the corresponding relative errors after calibration.

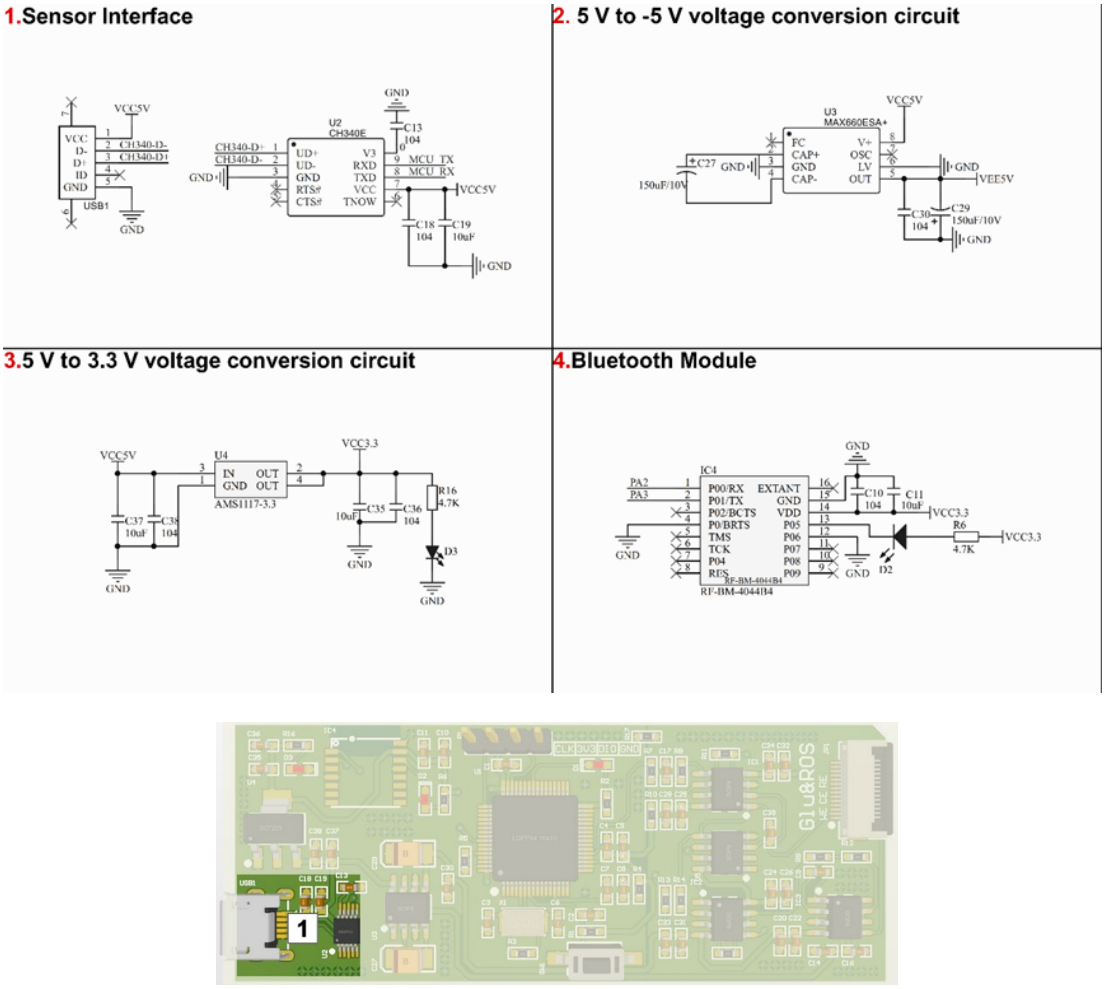

Figure S5. Circuit diagram showing the USB Serial Port (Circuit Component#1) of MAA. CH340E chip was utilized to connect the USB serial port and the printed circuit board. Powered by the computer serial port, the USB serial module was able to provide a stable voltage at 5V to the PCB for regular function. The module implemented communication interchange between the printed circuit board and the host computer, making it easy to adjust and validate the circuit design.

Figure S6. Circuit diagram showing the 5V to -5V voltage conversion circuit (Circuit Component#2) of MAA. In the lower circuit, 5V voltage supplied by the USB serial port was converted into a stable voltage at -5V through the MAX660ESA+ chip by the 5V to -5V module to ensure the regular function of the operational amplifier. The tantalum capacitor can filter and reduce the noise of the voltage signal, as well as storing energy.

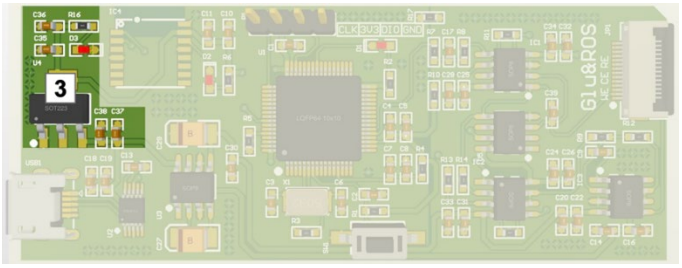

Figure S7. Circuit diagram showing the 5 V to 3.3 V voltage conversion circuit (Circuit Component#3) of MAA. In the 5 V to 3.3 V module, 5 V voltage supplied by the USB serial port was converted into a stable voltage at 3.3 V through the AMS1117-3.3 chip to ensure the regular function of the Bluetooth and the STM32 minimal system module.

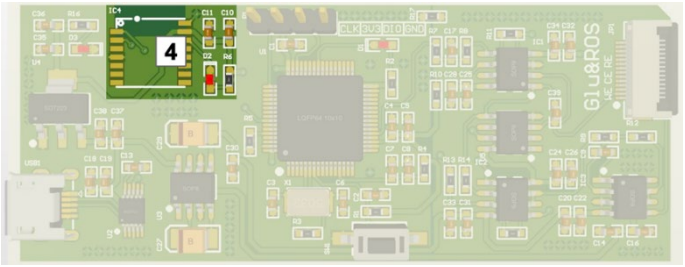

Figure S8. Circuit diagram showing the Bluetooth module (Circuit Component#4) of MAA. The main body was an integrated RF-BM-4044B4 low-power Bluetooth RF module. The module connected the hardware circuit with the host computer to achieve the function of highly integrated wireless communication, which was able to transfer the information collected by the circuit to the host computer conveniently.

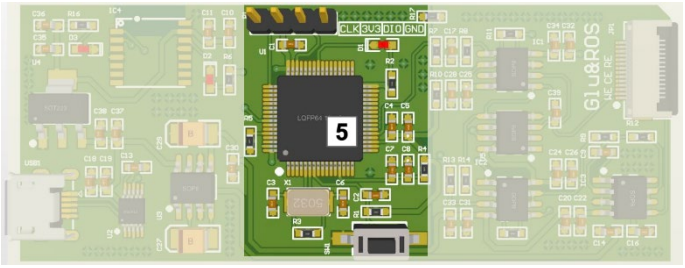

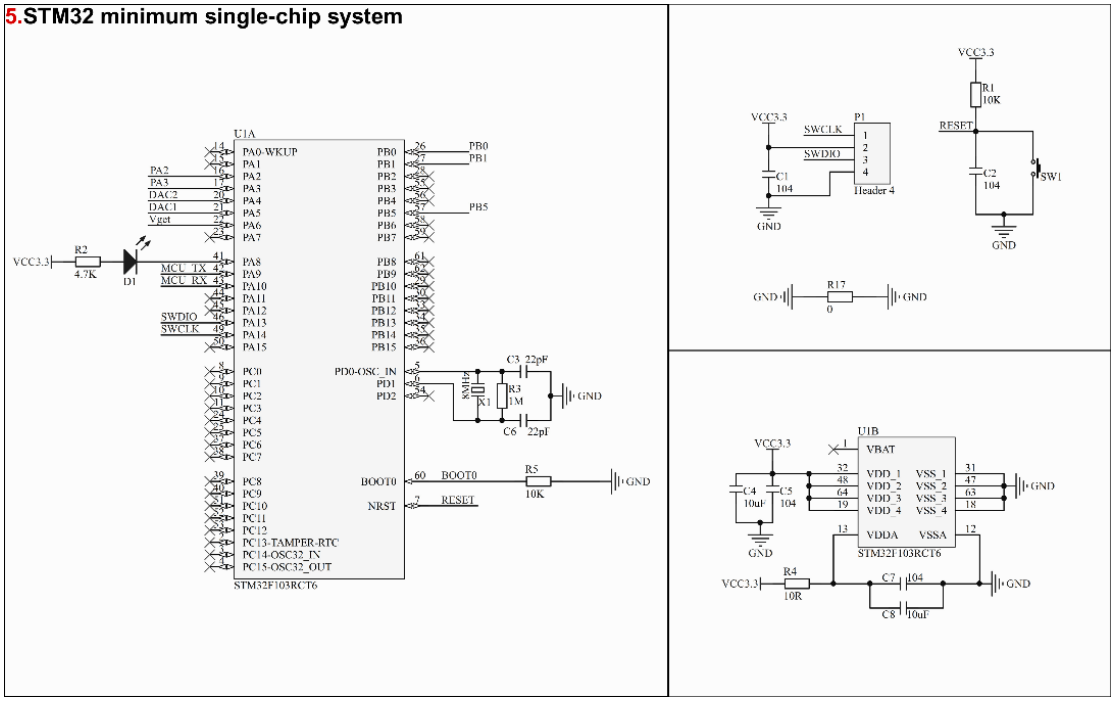

Figure S9. Circuit diagram showing the Minimum system module (Circuit Component#5) of MAA. This module is the minimum system module of the microcontroller. We call the resources in the STM32F103RCT6 master chip reasonably to realize the functions of data sending, data receiving and system resetting.

The minimum system module consisted of

1) Power supply, i.e., the 5V to 3.3V circuit mentioned above. This part provided a stable power supply at 3.3V to ensure the regular function of the chip;

2) Crystal oscillator circuit, to provide a precise clock signal required for the function of the system through the 8M external crystal oscillator;

3) Download circuit, this part implemented the program download in STM32, which could quickly overwrite and rewrite the program functions in the chip through the ST-link interface;

4) Reset circuit, the module was set to reset the program by pressing the reset button;

5) Data transfer, this part contained the data transfer between the circuit modules and transfer between the circuit board and the upper computer.

The data transfer between the circuit modules included: by calling the DAC and ADC modules in the chip, the test circuit was provided with the voltage signal required for regular function and converting the signals collected by the test circuit into digital signals to be parsed by the host computer. Data transfer between the circuit board and the host computer: different pins of the chip were call to send data through the USB serial port or Bluetooth module.

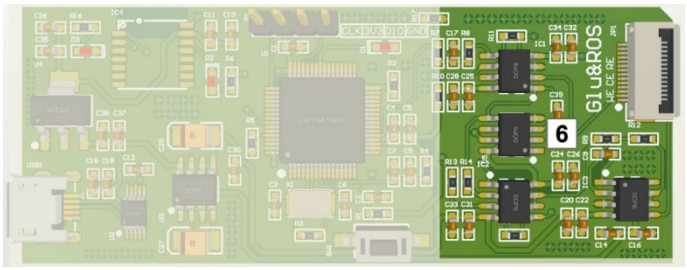

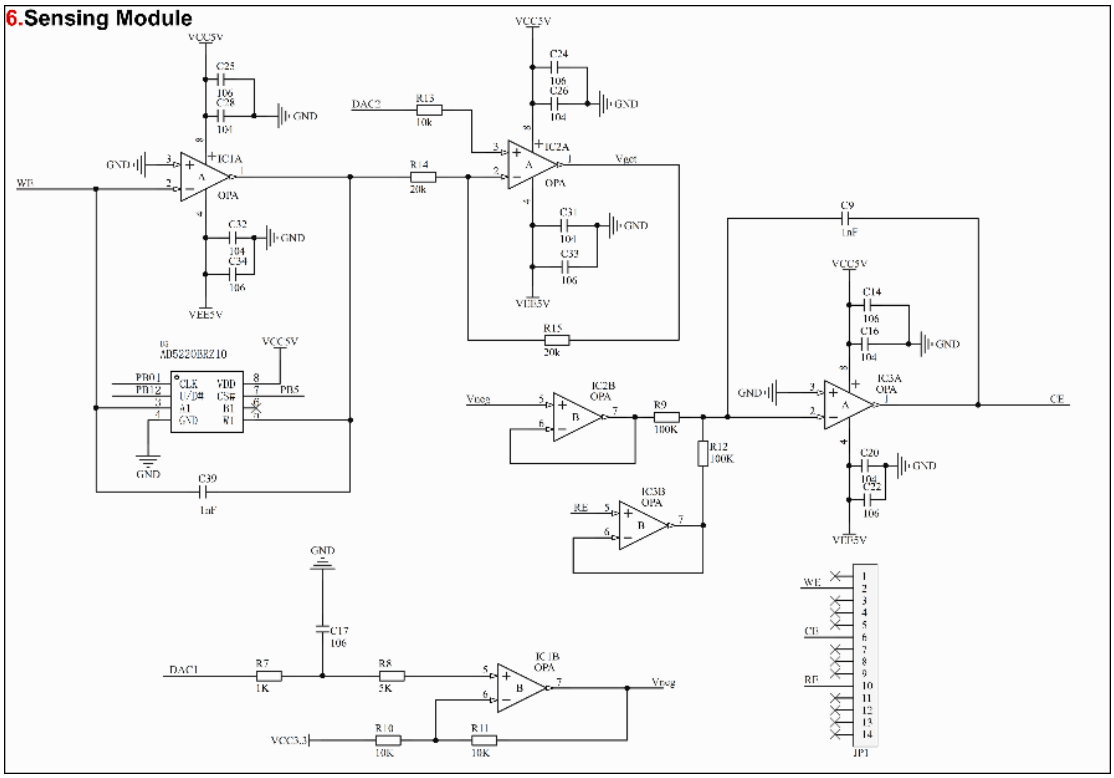

Figure S10. Circuit diagram showing the sensing module (Circuit Component#6) of MAA. This module was a three-electrode circuit for signal acquisition and processing, which could be utilized for electrochemical sensing of glucose or H_2O_2. Since the working voltages required during metabolite-test were different, a constant reference voltage in the detection circuit was need according to the electrochemical sensing principle. Therefore, the addition and subtraction operation circuit were first used to convert the positive voltage from STM32 chip into the stable negative voltage (or positive voltage) required by the post-stage circuit through deep negative feedback. Secondly, the stable voltage was put into the voltage follower of the post-stage to obtain a stable voltage applied to the reference electrode that can resist external interference effectively.

In the three-electrode system, a current loop was formed between the counter and working electrode by adjusting the control amplifier to provide the counter electrode a voltage of opposite phase to the reference electrode. In this way, a larger current could flow in the loop of the counter electrode.

For the working electrode, the current signal was converted into a corresponding voltage signal by means of a transimpedance amplifier. To realize the resistance conversion of the transimpedance module, AD5220 chip was used instead of the resistor of the transimpedance module. The resistance conversion of this chip was controlled by outputting the level signal through the specified pins of the MCU, making the

transimpedance module applicable to a larger data acquisition range. Finally, we output the adjusted voltage signal through the post-stage addition and subtraction operation circuit (for the current need to carry out the voltage lift), and the signal was acquired by the MCU.

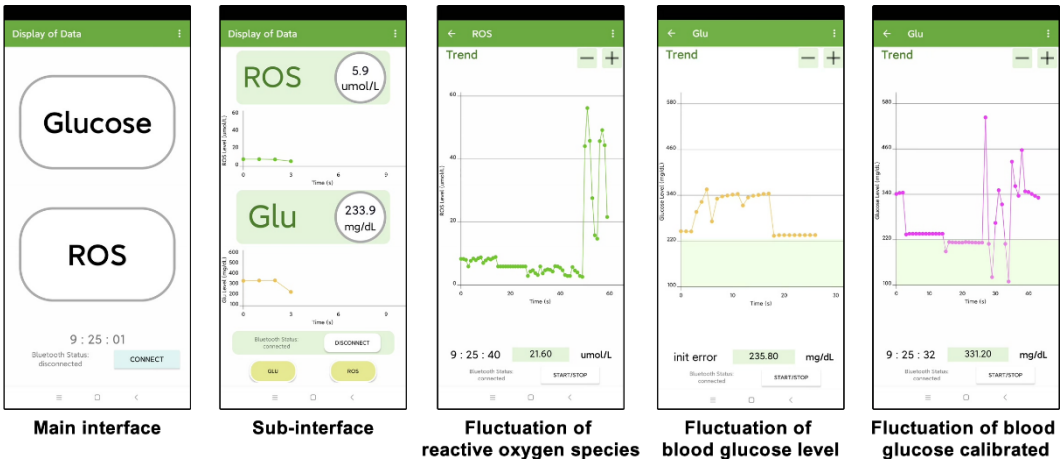

Figure S11. The photo showed the detailed interface of the app design on a smartphone, which be further developed. It shows the function of converting the signal to H_2O_2 and glucose concentration based on the current measured by the sensor and tracking it in real time.

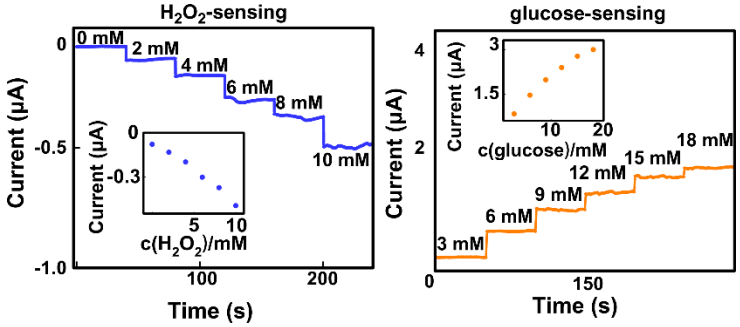

Figure S12. Graphs showing the current response of H_2O_2 and glucose collected with the metabolite-sensing micro-arrow electrode connected to the printed circuit board, respectively. The figures above displayed the current signal and time using MAA with the as-prepared printed circuit board.

Left: the current signal of the micro-arrow electrode processed an excellent linear relationship with the concentration of H_2O_2 with a detection sensitivity of 41.69 μA/mM (R^2= 0.981). Right: the current signal of the micro-arrow electrode exhibited a good linear relationship with the glucose concentration with a detection sensitivity of 13.72 μA/mM (R^2= 0.970).

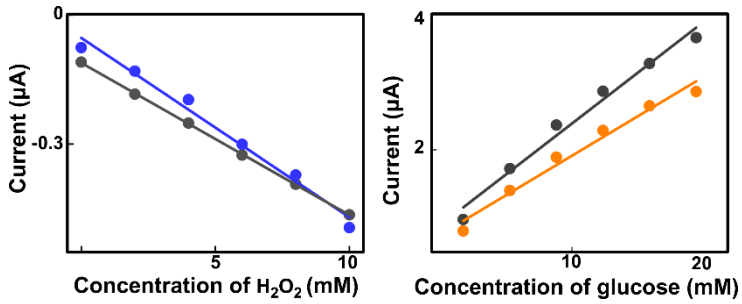

Figure S13. Graphs showing the relationship between the current signal on the metabolite sensing electrode using the as-prepared PCB and the commercial electrochemical workstation (ECW). The graph shows the variation of current with time using the as-prepared PCB compared to the ECW (black line).

The current signal of the H_2O_2-sensing micro-arrow electrode has a good linear relationship with the concentration of H_2O_2, with a detection sensitivity of 41.69 μA/mM (R^2= 0.981) for the prepared PCB and 35.37 μA/mM (R^2= 0.999)for the ECW. The current signal of the glucose sensing micro-arrow electrode had a good linear relationship with the glucose concentration, and the detection sensitivity was 13.72 μA/mM (R^2= 0.970) for the prepared PCB and 17.68 μA/mM (R^2= 0.976) for the ECW.

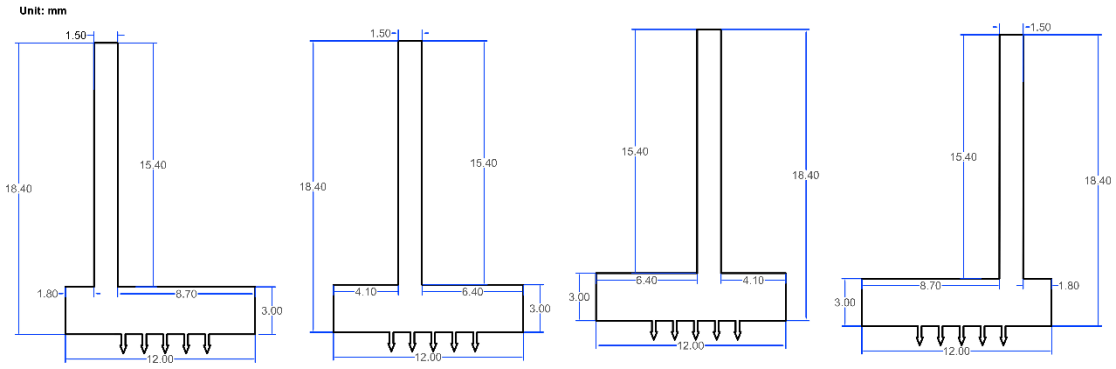

Figure S14. Graph of the micro-arrow electrode patches designed by AutoCAD. Each electrode contains five micro-arrow electrode tips with micro arrows of approximately 800 μm in length, a form back for fabricating microneedle arrays and a lead up to 15.4 mm long, which is suitable for bending, for integration and connection to a printed circuit board for stable data transfer.

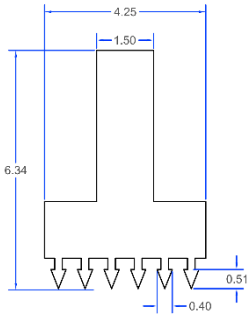

Figure S15. Graph of the micro-arrow electrode patches designed by AutoCAD for performing mechanical characterization. Each electrode contains six micro-arrow tips with a length of approximately 800 μm and micro-arrow tips with a barb structure of approximately 400 μm width to highlight the barb structure.

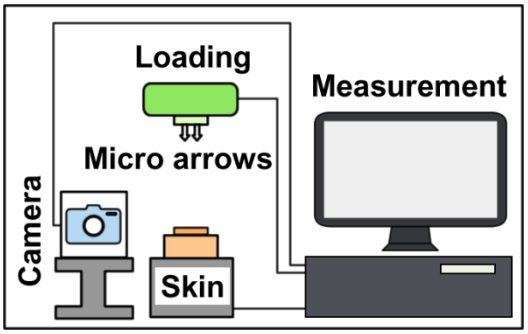

Figure S16. Image shows the experimental schematic of the puncture force measurement of the micro-arrow electrodes. In vitro experiments were performed using porcine skin as a simulation of human skin. The micro-arrow electrode tip was fixed vertically downward on the fixture of the puncture force measurement machine as well as being placed vertically directly above the fixed skin. Then, the micro-arrow electrode tip was pressed vertically onto the surface of the fresh pig skin by applying pressure from top to bottom, with a moving rate of 3 mm per second until lancing into the pig skin. After standing for 30 s, the tip was removed along the original path until the micro-arrow electrode was completely separated from the skin. The changes of the penetration force were recorded with a penetration force measurement machine to verify the adhesion of the micro structure of micro arrows during the process. Additionally, the entire process of needle entry and detachment from the skin was recorded with a camera for instant and visual observation.